Dimensional Control of Cobalt-hydroxide-carbonate Nanorods and Their Thermal Conversion to One-Dimensional Arrays of Co_3O_4 Nanoparticles

Rong Xu[†,‡] and Hua Chun Zeng*[,†]

Department of Chemical and Environmental Engineering, Faculty of Engineering, National University of Singapore, 10 Kent Ridge Crescent, Singapore 119260, and Institute of Chemical and Engineering Sciences, #02-08, Block 28, Ayer Rajah Crescent, Singapore 139959

Received: June 20, 2003

We report a detailed investigation on the formation of cobalt-basic-carbonate compounds $[Co(OH)_x(CO_3)_{0.5(2-x)}\cdot nH_2O]$ with dimensional and morphological controls. Two complementary precipitation methods developed in this work produce cobalt-basic-carbonate in the form of nanorods across a wide diameter span from 2 to 200 nm and a length up to 5 μm. Various controlling parameters were examined, such as anions in starting reagents, reaction temperature, aging time, and chemical compositions between the solid products and starting reagents. The resultant solids were characterized using XRD, FTIR, CHN, and TGA/DrTGA methods with respect to their formation process and thermal decomposition. More importantly, morphological aspects of the $Co(OH)_x(CO_3)_{0.5(2-x)}\cdot nH_2O$ and their heat-treated product Co_3O_4 were investigated with TEM/ED methods. It has been found that the $Co(OH)_x(CO_3)_{0.5(2-x)}\cdot nH_2O$ nanorods are grown along the [010] direction (orthorhombic). Upon thermal decomposition at $\geq$300 °C, the above nanorods self-assemble into one-dimensional arrays of Co_3O_4 nanoparticles along the [111] axis (cubic) of the spinel. Co_3O_4 nanorods can be prepared with this method in a small diameter regime of 20−40 nm.

Introduction

Monometal or mixed-metal basic salts have been extensively studied over the last two decades due to the important electric, magnetic and catalytic properties of their metal oxides formed upon thermal decomposition.[1−9] Cobalt oxides or cobalt-containing mixed oxides with spinel structure, $Co_{3-x}M_xO_4$ (M = Mg, Cu, Ni, Zn, etc), are active catalysts for oxidation reactions, as well as functional materials for oxide electrodes in electrochemical applications.[10−17] Among the various hydroxide-salt precursors for the cobalt spinels, hydroxide carbonates are more desirable, because there are no toxic product gases, such as nitrogen oxides from hydroxide nitrates,[18] and hydrochloric acid from hydroxide chlorides,[4] evolving during their decompositions.

The synthesis of the metal-hydroxide-carbonates $[M(OH)_x(CO_3)_{0.5(2-x)}\cdot nH_2O]$ usually involves coprecipitation of metal salts with an alkaline carbonate at constant pH in the range of 7 to 9.[6−9] In recent years, many of these research activities were devoted to synthesis of precursor compounds with highly dispersed cationic species, and investigations of their thermal decomposition behaviors. As a result, a substantial amount of information is now available on crystallography, structural chemistry, thermal reactivity, and surface properties of both the precursors and thermally decomposed oxide-materials. Compared to the above topical areas, nonetheless, much less attention has been paid to their dimensional and morphological controls and fabrication of nanoparticles from this class of compounds, although it has been well conceived that novel electrical, optical, magnetic and mechanical properties which could be realized by reducing crystallite dimensions to the quantum confinement regime.[19−21]

To achieve controlled fabrication of nanomaterials by precipitation methods, fundamental aspects on synthetic conditions and process parameters need to be investigated, which includes precipitation mode (e.g., either heterogeneous or homogeneous), reaction temperature and time, concentrations of starting reagents, type of counteranions, etc. To the best of our knowledge, however, there is no report which describes the effects of these control parameters on the morphological aspects of metal-basic-carbonates, despite two pioneering reports on the stated topics.[9,22] More specifically, a homogeneous precipitation of cobalt nitrate or sulfate by urea hydrolysis had yielded needle-type crystallites of cobalt-hydroxide-carbonates with a diameter ranging from a few tens to a few hundred nm and a length up to 10 μm.[22] Later, a study on the heterogeneous precipitation had also been carried out by reacting cobalt and zinc nitrates with ammonium carbonate in aqueous solution.[9] The resultant hydroxide-carbonates consisted of irregular particles of a few hundred nanometer for zinc-hydroxide-carbonate and around 100 nm for cobalt-hydroxide-carbonate compound.[9] Nonetheless, none of the above reports carried out a detailed investigation on dimensional/morphological controls of cobalt-hydroxide-carbonate compound precursors as well as their thermally converted oxide products.

In this work, therefore, we report our recent effort in morphological control of cobalt-basic-salts and their subsequent thermal conversion to low-dimensional nanostructured oxide materials. In particular, monodispersed nanorods of cobalt-basic-carbonate compounds have been prepared with a wide range of sizes by varying synthetic parameters, and the thermal conversion of these designed nanorod precursors to the one-

* Author to whom correspondence should be addressed. Tel: +65 874 2896. Fax: +65 779 1936. E-mail: chezhc@nus.edu.sg.
[†] National University of Singapore.
[‡] Institute of Chemical and Engineering Sciences.

10.1021/jp035751c CCC: $25.00
Published on Web 10/28/2003

TABLE 1: Samples Nomenclature and Experimental Conditions

sample	precipitation agent	counteranion	temperature (°C)	aging time (h)
A1	NaOH & Na_2CO_3	Cl^-	25	1
A2	NaOH & Na_2CO_3	Cl^-	25	22
A3	NaOH & Na_2CO_3	Cl^-	80	1
A4	NaOH & Na_2CO_3	Cl^-	80	22
A5	NaOH & Na_2CO_3	Cl^-	95	1
B1	urea	NO_3^-	95	2
B2	urea	NO_3^-	95	20
B3	urea	Cl^-	95	2
B4	urea	Cl^-	95	20

dimensional arrays of spinel Co_3O_4 nanoparticles has been achieved for the first time.

Experimental Section

Materials Preparation. Cobalt-basic-carbonate compounds were prepared by two types of precipitation methods. Samples series A (A1−A5) were synthesized by adding a mixture of 22.0 mL of 0.3 M NaOH aqueous solution (Fluka, > 98.0%) and 0.35 g of Na_2CO_3 (Merck, 99.9%) dropwise into 20.0 mL of 0.33 M $CoCl_2 \cdot 6H_2O$ aqueous solution (Fluka, >99.0%) within 40 to 50 min. The as-formed precipitate was aged in the mother liquor for either 1 or 22 h. During both addition and aging periods, the mixture was vigorously stirred and purged with purified N_2 (Soxal, 99.9995%) at 50 mL min^{-1}. The synthesis temperature was varied at 25, 80, and 95 °C, respectively, and they were kept constant throughout both precipitation and aging periods. Sample series B (B1−B4) were obtained using homogeneous precipitation method by urea hydrolysis. In this method, 20.0 mL of an aqueous solution of either $Co(NO_3)_2 \cdot 6H_2O$ (Fluka, >98%) or $CoCl_2 \cdot 6H_2O$ at 0.33 M was mixed with 4.0 g of urea (Merck, >99.5%). The mixture was kept in a screw-tight capped bottle which was then put in the oven preset at 110 °C for 2 or 20 h. The actual stable temperature of the reaction mixture was 95 °C, which was measured immediately after taking out the bottle at the end of the reaction. Finally, all the precipitates were washed by centrifuging with a large amount of deionized water to remove any impurities. Each washed precipitate was then dried in an oven at 50 °C overnight. Table 1 summarizes the synthesis parameters for all the samples.

The two series of samples were further heat-treated in static air. The calcination temperatures were set above those at which the stable weight was obtained in TGA measurements (see the below part). For example, the calcination temperatures for sample B1 were varied at 300, 400, 500 °C and for sample B3 was at 400 °C. In each experiment, around 200 mg of as-prepared samples was calcined at the selected temperatures for 3 h with the heating rate fixed at 2 °C min^{-1}.

Materials Characterization. The crystallographic information of prepared samples was analyzed by powder X-ray diffraction (XRD) method using a Bruker AXS diffractometer with Cu Kα radiation ($\lambda = 1.5406$ Å) at a scanning rate of 1° min^{-1}. Chemical bonding information on metal−oxygen, metal−anions, and hydroxyl were studied with Fourier transform infrared spectroscopy (FTIR, Bio-Rad) using a potassium bromide (KBr) pellet technique. Each FTIR spectrum was collected after 40 scans at a resolution of 4 cm^{-1} from 400 to 4000 cm^{-1}. The weight percentage of carbon in the prepared samples was measured in a EURO EA elemental analyzer. Thermal behavior of samples was analyzed out using thermogravimetric method (TGA) in a TA instrument SDT-2960. About 10−11 mg of the samples was heated with an air flow of 100 mL min^{-1} and at a heating rate of 10 °C min^{-1} from room temperature to 600 °C. Morphologies and structures of the as-synthesized samples as well as their calcined samples were investigated using a JEM-2010 transmission electron microscope (TEM; together with electron diffraction (ED) experiments) with a LaB_6 electron gun and an electron kinetic energy of 200 kV. For specimen preparation, around 5 mg of the wet precipitates A1−A5 (after washing and before drying) and 3 mg of dry samples B1−B4 and calcined B1 and B3 were dispersed into approximately 15 mL of acetone, and the resultant mixture was then treated with ultrasound radiation for 1 h. A few drops of ultrasonicated mixture were then spread onto a commercial copper grid coated with amorphous carbon layers and Formvar film, followed by a drying treatment at 60 °C.

Results and Discussion

Figure 1, parts a and b, shows the XRD patterns of as-prepared samples. In Figure 1a, the weak diffraction intensities indicate that samples A1−A5 prepared with the heterogeneous precipitation (by adding NaOH and Na_2CO_3 directly into a $CoCl_2$ solution) were not well crystallized and the particle size should be small, especially for the samples prepared at 25 °C (A1 and A2). Samples synthesized at higher temperatures have a better crystallinity, while aging time shows little effect on the crystallinity (Figure 1a; A1 vs A2, and A3 vs A4; also see Table 1 and Figure 4a). The XRD patterns all show characteristics of the cobalt-basic-carbonate phase, which is in good agreement with a reported compound, $Co(OH)_{1.0}(CO_3)_{0.5} \cdot 0.11H_2O$, with lattice constants $a = 8.79$ Å, $b = 10.15$ Å, and $c = 4.43$ Å (space group $P22_12$).[8] The *hkl* reflections shown in Figure 1a can be indexed perfectly to this orthorhombic solid compound.[8]

In the previous work,[8] cobalt-basic-carbonate compound was obtained by a constant pH precipitation of cobalt salt with $NaHCO_3$. Similar results were also obtained in recent years,[9,23] where ammonium carbonate was used as a precipitation agent.[23] Since the molar ratio of $Co^{2+}/OH^-/CO_3^{2-}$ in our starting solutions is 1:1:0.5, which is identical to the stoichiometric requirement of this compound, it is not surprising that the compounds formed match the reported XRD pattern. Upon the addition of OH^- and CO_3^{2-} anions into the $CoCl_2$ solution, the following reaction should take place:

$$Co^{2+} + xOH^- + 0.5(2-x)CO_3^{2-} + nH_2O \rightarrow Co(OH)_x(CO_3)_{0.5(2-x)} \cdot nH_2O \quad (1)$$

Due to its complexation ability with cobalt, however, Cl^- anions present in the metal solution could also be incorporated into the precipitates to form basic chlorides $[Co(OH)_xCl_{2-x} \cdot nH_2O]$,[4,24] or chloride-containing basic carbonate compounds $[Co(OH)_x Cl_y(CO_3)_{0.5(2-x-y)} \cdot nH_2O]$.[25] The former compounds usually have a well-crystallized hexagonal structure, while the latter retain the same orthorhombic phase of cobalt-basic-carbonate. We had found that when an insufficient amount of NaOH and Na_2CO_3 was added, the resulted precipitate was in fact a mixture of cobalt-basic-carbonate and basic-chloride compounds (confirmed by the XRD method; not shown). Except the cobalt-basic-carbonates, other possible precipitates, such as $Co(OH)_2$, $CoCO_3$, and $Co(OH)_xCl_{2-x} \cdot nH_2O$, were not detected (verified by XRD analysis). The formation of chloride-containing basic-carbonates could also be ruled out,[25] on the basis of our FTIR analysis (in Figure 2).

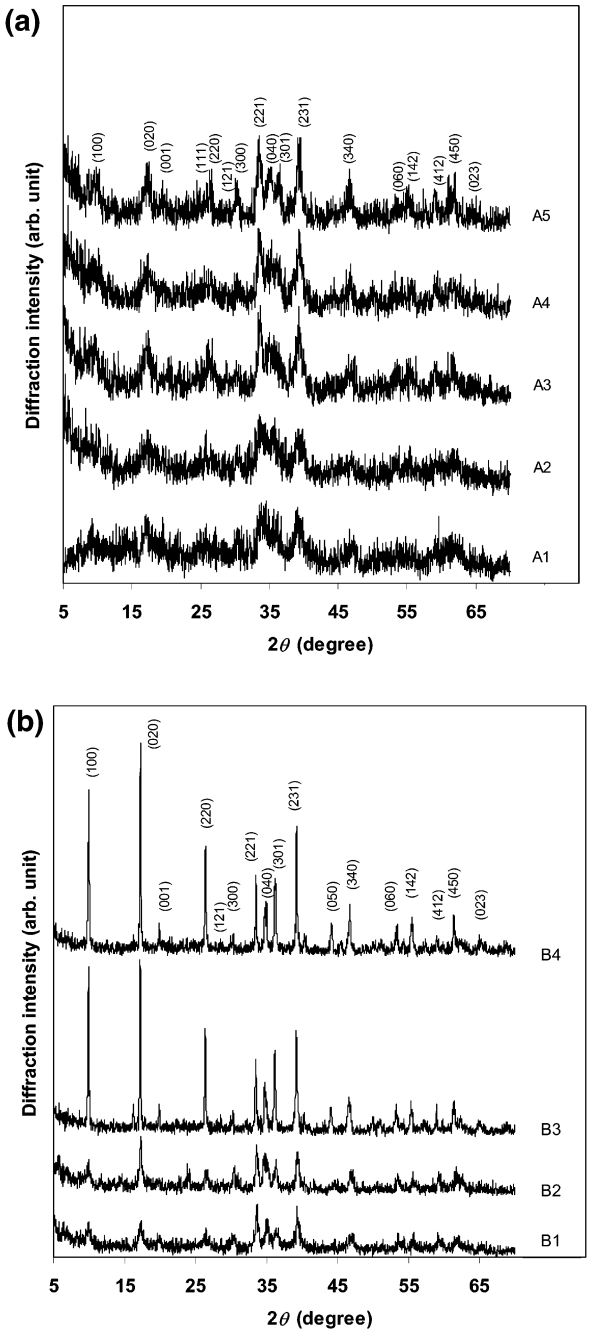

Figure 1. (a) XRD patterns of as-prepared cobalt-hydroxide-carbonate compounds, A1−A5, by heterogeneous precipitation method using NaOH and Na_2CO_3. (b) XRD patterns of as-prepared cobalt hydroxide carbonate compounds, B1−B4, prepared by a homogeneous precipitation method using urea.

With the homogeneous precipitation, the crystallinity can be improved further, as shown in samples B1−B4 of Figure 1b (where the urea hydrolysis provided both carbonate and hydroxyl anions to react with cobalt cations), especially for those synthesized with the $CoCl_2$ (B3 and B4). As an example, our XRD analysis indicates that the lattice constants for B4 (a = 8.72 Å, b = 10.29 Å, and c = 4.45 Å) agree very well with the literature data.[8] In this precipitation, a sudden burst of nuclei occurred when the temperature was raised and the nuclei subsequently were grown into larger crystallites by an aggregation mechanism.[26,27] Compared to A1−A5, samples B1−B4 were much better crystallized (also see Figure 4b). The crystallinity of precipitates was also affected by the type of

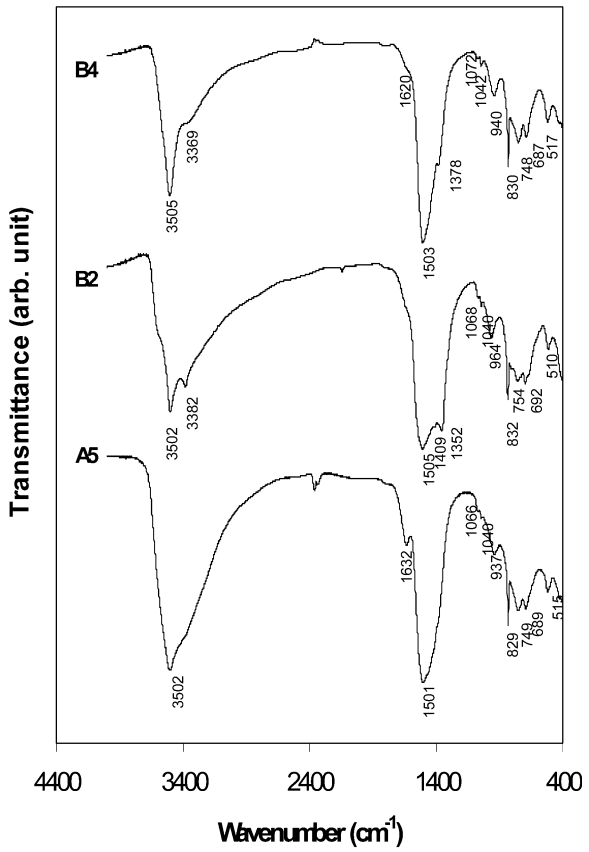

Figure 2. FTIR spectra of some representative as-prepared samples A5, B2, and B4.

counteranions present in the synthesis, as samples B3 and B4 (using $CoCl_2$) were clearly better crystallized than B1 and B2 [using $Co(NO_3)_2$].

Our FTIR investigation also affirms the formation of cobalt-hydroxide-carbonate. Figure 2 presents the FTIR spectra of samples A5, B2, and B4 (spectra of the samples A1−A4, B1, and B3 are not plotted here, since they are very similar to those of A5, B2, and B4, respectively). The strong peaks at 3502−3505 cm^{-1} are assigned to the stretching vibration of the O−H group of molecular water and of hydrogen-bound O−H groups,[28,29] noting that the peak at 1620−1632 cm^{-1} is due to the bending mode of water molecules.[6] The shoulder vibration appearing at around 3369−3382 cm^{-1} is attributed to the O−H groups interacting with carbonate anions. The strength of this shoulder component decreases in the order of A5 > B2 > B4, and is indeed proportional to the amount of carbonate anions incorporated, as verified by the elemental analysis results (Table 2). The presence of CO_3^{2-} in the samples is evidenced by its vibration bands from middle to lower wavenumbers, which suggests the presence of a mono- or poly-dentate carbonate ligand.[30,31] The bands observed at 1501−1505 cm^{-1} are assigned to stretching vibration $\nu(OCO_2)$, 1409 cm^{-1} (sample B2) to $\nu(CO_3)$, where the splitting of $\nu(OCO_2)$ and $\nu(CO_3)$ indicates the decrease of the symmetry from D_{3h} (for a free carbonate group) to C_{2v}. The sharp peak present in all the spectra at 829−832 cm^{-1} is attributed to $\delta(CO_3)$, and the rest of the minor bands at 1066−1072, 748−754, and 687−692 cm^{-1} can be assigned to $\nu(C{=}O)$, $\delta(OCO)$, and $\rho(OCO)$, respectively,[6] while the bands at 937−964 cm^{-1} are ascribed to $\delta(M-OH)$ bending modes while the band at 510−517 cm^{-1} is ascribed to $\rho_w(MOH)$. On the other hand, absorptions of Cl^-, NO_3^-, NH_3 or NH_4^+, and NCO^- or CN^- are not detected. Since FTIR analysis is a very sensitive technique, it can be concluded that

TABLE 2: TGA and Elemental Analysis Results for As-Prepared Cobalt Hydroxide Carbonates Samples

sample	wt_{H_2O}%[a]	wt_{total} %[b]	wt_c %[c]	formula	wt_{total} %[d]
A1	7.96	28.56	5.35	$Co(OH)_{0.98}(CO_3)_{0.51}\cdot 0.51H_2O$	30.27
A2	8.03	28.39	5.28	$Co(OH)_{0.98}(CO_3)_{0.51}\cdot 0.52H_2O$	30.17
A3	6.84	28.21	5.14	$Co(OH)_{1.02}(CO_3)_{0.49}\cdot 0.43H_2O$	29.81
A4	6.12	28.62	5.17	$Co(OH)_{1.04}(CO_3)_{0.48}\cdot 0.38H_2O$	29.79
A5	4.76	28.05	5.30	$Co(OH)_{1.02}(CO_3)_{0.49}\cdot 0.29H_2O$	29.88
B1	3.80	27.24	4.22	$Co(OH)_{1.24}(CO_3)_{0.38}\cdot 0.23H_2O$	28.01
B2	2.13	26.05	4.12	$Co(OH)_{1.28}(CO_3)_{0.36}\cdot 0.12H_2O$	27.73
B3	0.72	25.18	3.42	$Co(OH)_{1.42}(CO_3)_{0.29}\cdot 0.04H_2O$	26.52
B4	0.67	26.41	3.76	$Co(OH)_{1.36}(CO_3)_{0.32}\cdot 0.04H_2O$	27.06

[a] The weight percentage of H_2O obtained from weight loss data in TGA curve from room temperature to 150 °C. [b] The total weight loss percentage obtained from TGA data. [c] The weight percentage of carbon measured by CHN method. [d] The estimated weight loss percentage based on the obtained molecular formula.

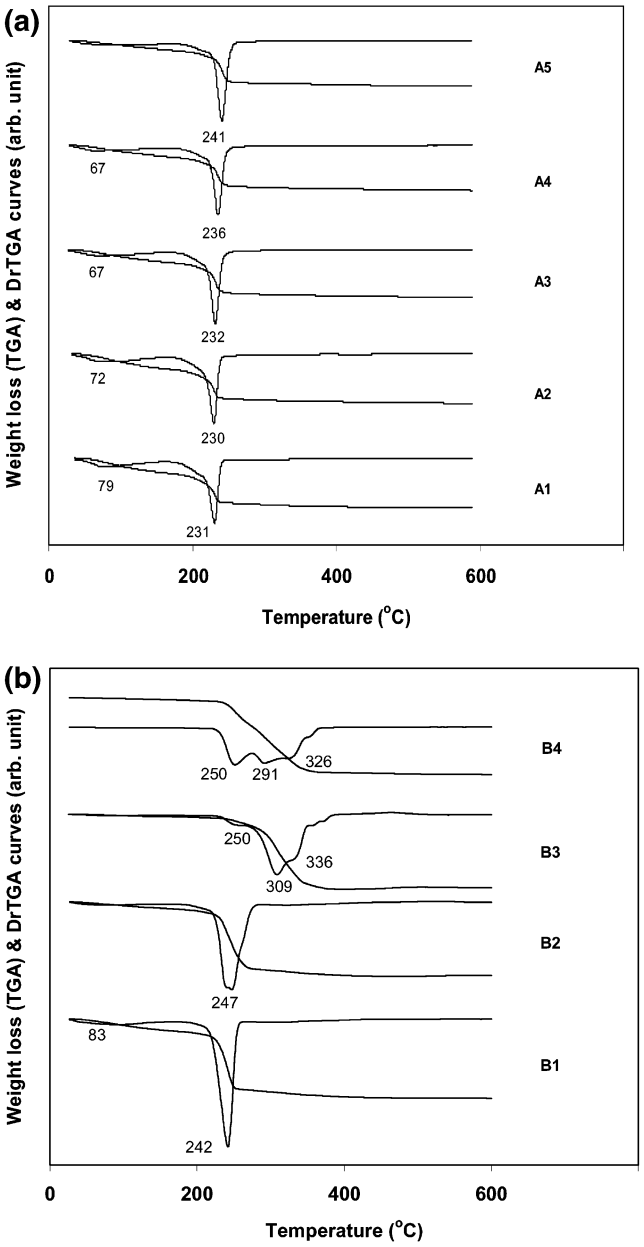

Figure 3. (a) TGA and DrTGA curves of samples A1−A5 (prepared by heterogeneous precipitation method using NaOH and Na_2CO_3), heating rate: 10 °C min^{-1}; air flow: 100 mL min^{-1}. (b) TGA and DrTGA curves of samples B1−B4 (prepared by a homogeneous precipitation method using urea), heating rate: 10 °C min^{-1}; air flow: 100 mL min^{-1}.

the CO_3^{2-} group is the only anion (from the salt reagents) incorporated in these samples.

In agreement with the FTIR results, our CHN analysis indeed confirms the absence of nitrogen in all the samples. Figure 3 reports the TGA and DrTGA curves for all the samples. Under air atmosphere, samples A1−A5 (Figure 3a) have similar thermal behaviors. The first weight loss is indicated by the broad bands centered at around 70 °C in DrTGA curves, due to the elimination of molecular waters in the materials. As the temperature increases, a well-defined peak at 230−241 °C in DrTGA curves can be observed owing to a simultaneous removal of structural water and carbon dioxide by dehydroxylation and decomposition of carbonate anions. The decomposition temperature increases with the synthesis temperature. In Figure 3b, however, samples B1 and B2 have very similar weight loss patterns (also see DrTGA curves; at 242 and 247 °C), whereas B3 and B4 decompose at several steps over 250 to 336 °C. This is understandable because the latter two were better crystallized (thermally more stable), and the dehydroxylation and decomposition of carbonate anions took place sequentially.

As summarized in Table 2, the calculated molar ratio of $Co^{2+}/OH^-/CO_3^{2-}$ in samples A1−A5 matches excellently with that set in the starting solutions, and the good agreement between the calculated and actual total weight loss percentages also validates the determined chemical formulas. It is interesting to note that the amount of carbonate anions in these samples decreases in the order of A1−A5 > B1−B2 > B3−B4, opposing the degree of crystallinity (Figure 1). A similar decreasing trend is also observed for the incorporated water.

The morphologies of the as-prepared solids as well as their calcined samples were examined with TEM method. In Figure 4a, the effect of synthesis temperature on the crystallite morphology is demonstrated. In accordance with the XRD results, A1 and A2 synthesized at 25 °C consist of aggregates of rodlike crystallites with the breadth of only 2−4 nm and the length of around 50 nm. Larger nanorods were formed when the temperature was increased, whereas little change is observed with an aging treatment. The nanorods synthesized at 80 °C (A3 and A4, Table 1) have a diameter of 5−8 nm and a length of 50−70 nm. When the temperature was further increased to 95 °C (A5, Table 1), the formed nanorods are getting larger with the diameters at 10−15 nm and the lengths at 120−180 nm. Owing to the nanoscale nature of A1−A5 samples; however, only weak diffraction rings (also see XRD, Figure 1a) can be observed from the ED patterns of the aggregates, as an example for sample A5, noting that all the samples have a good monodispersity (i.e., with a narrow size distribution).

Sample morphologies of B1−B4 prepared with the urea method are shown in Figure 4b. As expected, these samples consist of larger free-standing crystallites and the effect of counteranions on the morphology can also be noticed. Both B1

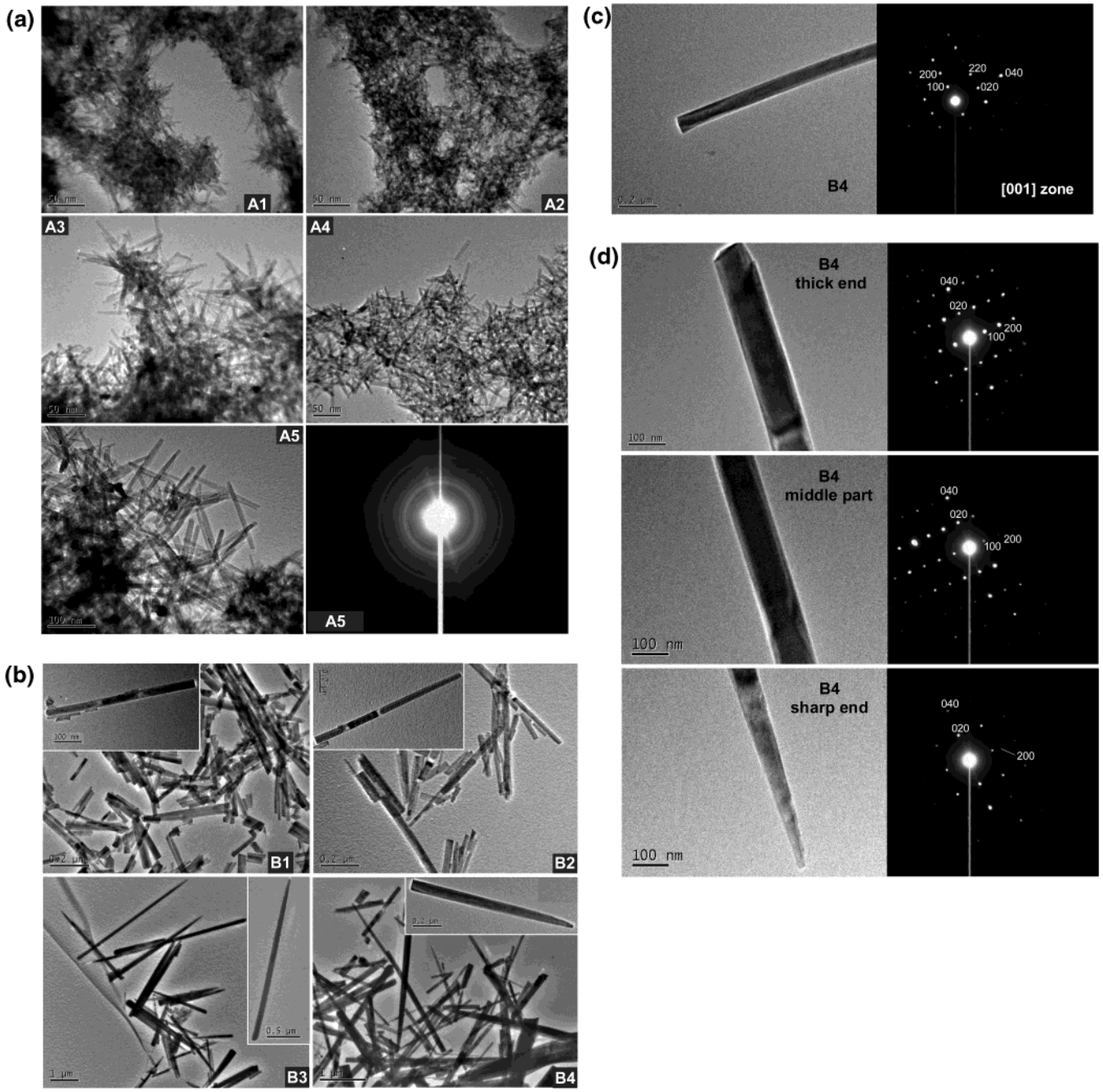

Figure 4. (a) TEM images for samples A1−A5 (prepared by a heterogeneous precipitation method using NaOH and Na_2CO_3) and ED pattern for sample A5. (b) TEM pictures for samples B1−B4 (prepared by a homogeneous precipitation method using urea) and the free-standing nanorod for each sample (inserts). (c) TEM image and ED pattern of a free-standing nanorod selected from sample B4 (prepared by a homogeneous precipitation method using urea at 95 °C for 20 h). (d) Selected area ED patterns of the three different parts (two ends and the middle) of a free-standing nanorod selected from sample B4 (prepared by a homogeneous precipitation method using urea at 95 °C for 20 h).

and B2 exhibit square-ended nanorods of cobalt-basic-carbonate with a constant diameter of around 50 nm and a length up to 1−2 μm. Samples B3 and B4, on the other hand, have a needlelike morphology with a reducing diameter at the tip. The dimensions of latter crystallites are typically within a diameter range of 100 to 200 nm and a length range of 1 to 5 μm. Similarly, the effect of aging time is not obvious for this sample series either, as had been affirmed with other characterization methods.

Selected area ED analysis was carried out to study the crystallographic orientations of the above rod-shaped crystallites. Figures 4c and 4d display ED patterns of two free-standing nanorods from sample B4 that shows the best crystalline features among the studied samples. In Figure 4c, the orthorhombic diffraction pattern can be indexed into *hk*0 spots, and the lattice constants (*a* and *b*) obtained from the ED pattern are in excellent agreement with those from the XRD method, noting that the electron beam was injected perpendicular to the (001) plane of the crystal. Therefore, the single-crystal nature of these nanorods and their growth direction along [010] are elucidated. In Figure 4d, both the thick end and the middle part of the rod exhibit the same diffraction pattern. However, the ED pattern of the sharp end is different. While the original *0k*0 spots may be still recognizable, the *h*00 and other *hk*0 spots are hardly traceable. The emerging new spots (square-like) suggests that the tip of this nanorod has been undergoing structural changes in the radial direction (i.e., [100]) of the nanorod upon the electron beam irradiation. This observation is in general agreement with the

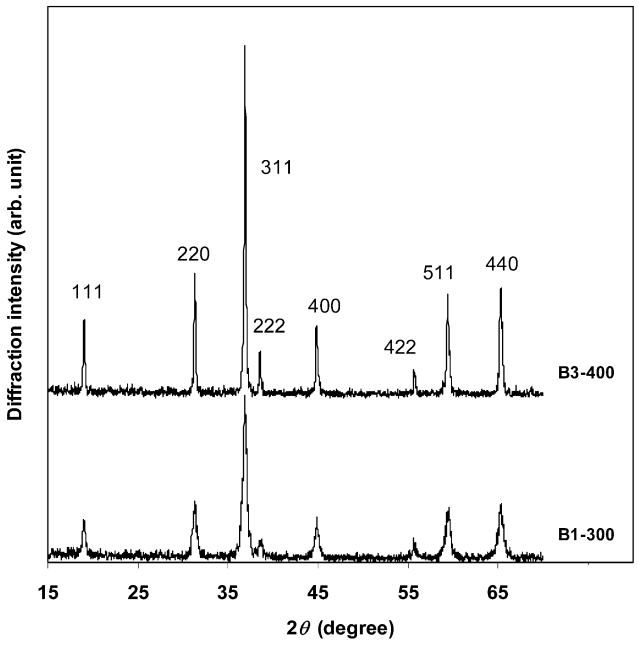

Figure 5. XRD patterns of calcined samples in static air, B1-300 (heating rate: 2 °C min^{-1}; calcination temperature and time: 300 °C and 3 h) and B3-400 (heating rate: 2 °C min^{-1}; calcination temperature and time: 400 °C and 3 h).

low thermal/chemical stability observed in the TGA/DrTGA study for this compound.

It is well-known that the precipitation of cobalt cations and a base usually generates cobalt-hydroxides which are known to crystallize in two polymorphic forms, namely α- and β-cobalt-hydroxides. While α-$Co(OH)_2$ is a metastable phase (it normally transforms to the β-form during synthesis),[29] the β-$Co(OH)_2$ phase is usually formed into large hexagonal crystal platelets with high crystallinity. As mentioned earlier, the homogeneous precipitation method using urea generated cobalt compounds in the shape of nanorods or needles in a *closed* system.[22] Samples obtained with an open system described in the same report had platelet-like morphology. This is most probably due to the fact that the amount of carbonate anions in a closed system during the urea decomposition is more predominant than that in the open system, from which carbonate group was released in the form of gaseous CO_2. In the current work, carbonate anions together with sodium hydroxide were added directly into the metal solution. Similar rodlike nanostructures but in much smaller size can be controlled in A1−A5 experiments. Though they are essential for the formation of basic carbonate compounds, the carbonate anions may also act as an inhibitor that selectively decreases the rates of crystal growth along both [001] and [100] directions, resulting in the [010]-elongated nanorods. In an earlier report, cobalt nitrate solution (1 M) and ammonium carbonate solution (2 M) were simultaneously pumped into a mixing vessel at 70−75 °C (constant pH precipitation method).[9] Although the XRD result indicated the formation of cobalt-basic-carbonate compound, the TEM analysis showed that the formed crystallites were irregularly shaped.[9] This difference in product morphologies may be attributable to the different precipitation and experimental conditions. In addition to cobalt-basic-carbonate, goethite (α-FeOOH) crystallites had been obtained in the nanometer regime with an elongated shape (aspect ratio from ∼5 to ∼8) by adding Na_2CO_3 into an $FeSO_4$ solution, despite lack of proposed formation mechanisms.[32]

Upon the calcination at ≥300 °C, all the cobalt-basic-carbonate compounds prepared in this work were converted into the oxide Co_3O_4. Displayed in Figure 5, for example, the as-prepared B1 and B3 were transformed completely to the cubic-phase spinel Co_3O_4, as indicated by the XRD patterns (B1-300 and B3-400). The morphologies of all the calcined samples are reported in Figure 6. The TEM images (Figure 6a) indicate that after the calcination the pristine cobalt-basic-carbonate nanorods were transformed into strings of Co_3O_4 nanoparticles (or "beads") interconnected along the original longitudinal directions of the rods. As revealed in our TGA/DrTGA results (Figure 3), during the thermal decomposition, the elimination of hydroxyl and carbonate groups and the formation of new crystalline phase caused the disruption of the original rodlike morphology and led to the 1D beadlike-assemblies. It is observed that higher calcination temperatures generated larger crystallites [Figure 6a, (a), (b), and (c)]. Selected area ED patterns (Figure 6b) reveal that the Co_3O_4 subunits along the rods have a predominant assembling direction of [111], because the intensities of *hkl* diffractions are much stronger compared with the rest. Furthermore, lattice fringes of d_{111} (0.46 nm) have been observed perpendicularly to the Co_3O_4 rods (not shown). Although Co_3O_4 is an antiferromagnetic material, a layer of ferromagnetic Co could be formed on the surface of this oxide spinel under an electron beam (such as in TEM measurements), which may cause a self-alignment of the small particles through weak

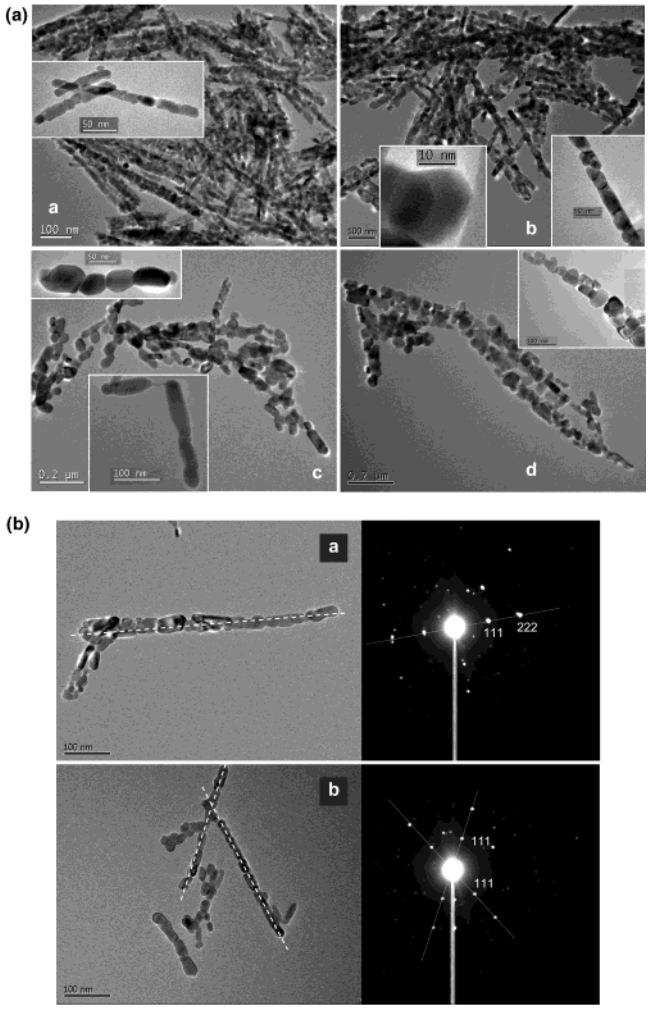

Figure 6. (a) TEM images of selected samples calcined at different temperatures (heating rate: 2 °C min^{-1}; heating time: 3 h): (a) B1-300, 300 °C; (b) B1-400, 400 °C; (c) B1-500, 500 °C, and (d) B3-400, 400 °C. (b) Two TEM images (a and b) of sample B1-400 (heated at 400 °C, 2 °C min^{-1}, 3 h) and their respective selected area ED patterns.

magnetic interactions. In addition, residual magnetic fields present in the measuring surroundings may introduce the paramagnetic effect for this alignment or aggregation. We had recently observed loose aggregates of Co_3O_4 nanocubes in a nonpermanent manner through these possible mechanisms under the TEM measurement conditions.[33,34] Using the nanorods of cobalt-basic-carbonate precursors, as demonstrated in this work, we are now able to assemble Co_3O_4 nanoparticles into permanent 1D-arrays. Very recently, Co_3O_4 nanorods with a diameter of 40−100 nm have been prepared by a molten salt synthesis at 800 °C.[35] In fact, the assembling arrangement of nanocrystals in the present study can also be viewed as a new way for the formation of Co_3O_4 nanorods. Although the two preparative methods are totally different, the [111] axis has been found to be the common rod axis (i.e., the growth direction) in all the two studies. Nonetheless, the diameter of the nanorods in our synthesis is much smaller (around 20−40 m) as shown in Figure 6, in complement to the reported diameter range.[35]

Conclusions

In summary, nanorods of cobalt-basic-carbonate compounds with size and morphological controls have been synthesized using two complementary precipitation methods. The samples obtained from the heterogeneous precipitation by adding NaOH and Na_2CO_3 aqueous solutions into $CoCl_2$ solution have monodispersed rodlike morphologies of less than 20 nm in diameter and less than 200 nm in length, depending on the synthesis temperature. The composition of the as-prepared compounds matches very well with the molar ratio of different species in the starting solutions ($Co^{2+}/OH^-/CO_3^{2-} = 1:1:0.5$). On the other hand, samples synthesized with the urea hydrolysis consist of larger well-crystallized nanorods, and the effect of counteranions in this experiment is significant. Samples obtained with $Co(NO_3)_2$ have a uniform diameter at around 50 nm and a length at 1−2 μm, whereas the samples with $CoCl_2$ show needlelike crystallites with a much larger size (100−200 nm in diameter, and 1−5 μm in length). All cobalt-basic-carbonate nanorods are grown along the [010] direction (orthorhombic phase). Upon the calcination at ≥300 °C, the above nanorods are transformed into cubic phase spinel oxide, Co_3O_4, giving away one-dimensional arrays of Co_3O_4 nanoparticles with the [111] axis along their assembling-axis. This method can be used for synthesis of Co_3O_4 nanorods with a small diameter in the regime of 20−40 nm.

References and Notes

(1) Xu, X.; Doesburg, E. B. M.; Scholten, J. J. F. *Catal. Today* **1987**, *2*, 125.

(2) Petrov, K.; Markov, L. *Silikattechnik* **1986**, *37*, 197.

(3) Fornasari, G.; Gusi, S.; Trifiro, F. *Ind. Eng. Chem. Res.* **1987**, *26*, 1500.

(4) Garcia-Martinez, O.; Millan, P.; Rojas, R. M.; Torralvo, M. J. *J. Mater. Sci.* **1988**, *23*, 1334.

(5) Baker, J. E.; Burch, R.; Golunski, S. E. *Appl. Catal.* **1989**, *53*, 279.

(6) Klissurski, D. G.; Uzunova, E. L. *Chem. Mater.* **1991**, *3*, 1060.

(7) Porta, P.; Dragone, R.; Fierro, G.; Inversi, M.; Lojacono, M.; Moretti, G. *J. Mater. Chem.* **1991**, *1*, 531.

(8) Porta, P.; Dragone, R.; Fierro, G.; Inversi, M.; Lojacono, M.; Moretti, G. *J. Chem. Soc., Faraday Trans.* **1992**, *88*, 311.

(9) Baird, T.; Campbell, K. C.; Holliman, P. J.; Hoyle, R. W.; Stirling, D.; Williams, B. P.; Morris, M. *J. Mater. Chem.* **1997**, *7*, 319.

(10) Jang, Y. I.; Wang, H.; Chiang, Y. M. *J. Mater. Chem.* **1998**, *8*, 2761.

(11) Langell, M. A.; Anderson, M. D.; Carson, G. A.; Peng, L.; Smith, S. *Phys. Rev. B* **1999**, *59*, 4791.

(12) Joseph, Y.; Ranke, W.; Weiss, W. *J. Phys. Chem. B* **2000**, *104*, 3224.

(13) (a) Angelov, S.; Mehandjiev, D.; Piperov, B.; Zarkov, V.; Terlecki-Baricevic, A.; Jovanovic, D.; Jovanovic, Z. *Appl. Catal.* **1985**, *16*, 431. (b) Klissurski, D.; Uzunova, E.; Yankova, K. *Appl. Catal. A* **1993**, *95*, 103. (c) Takada, T.; Kasahara, S.; Omata, K.; Yamada, M. *Nippon Kagaku Kaishi* **1994**, 793. (d) Omata, K.; Takada, T.; Kasahara, S.; Yamada, M. *Appl. Catal. A* **1996**, *146*, 255.

(14) Salker, A. V.; Gurav, S. M. *J. Mater. Sci.* **2000**, *35*, 4713.

(15) Carapuca, H. M.; Pereira, M. I. D.; Dacosta, F. M. A. *Mater. Res. Bull.* **1990**, *25*, 1183.

(16) Singer, J.; Fielder, W. L. *J. Power Sources* **1990**, *29*, 443.

(17) Fradette, N.; Marsan, B. *J. Electrochem. Soc.* **1998**, *145*, 2320.

(18) Petrov, K.; Zotov, N.; Mirtcheva, E.; Garcia-martinez, O.; Rojas, R. M. *J. Mater. Chem.* **1994**, *4*, 611.

(19) Henglein, A. *Chem. Rev.* **1989**, *89*, 1861.

(20) Brus, L. E.; Trautman, J. K. *Philos. Trans. R. Soc., London, Ser. A—Math. Phys. Eng. Sci.* **1995**, *353*, 313.

(21) Yoffe, A. D. *Adv. Phys.* **1993**, *42*, 173.

(22) Ishikawa, T.; Matijević, E. *Colloid Polym. Sci.* **1991**, *269*, 179.

(23) Fierro, G.; Dragone, R.; Moretti, G.; Porta, P. *Surf. Interface Anal.* **1992**, *19*, 565.

(24) Garcia-Martinez, O.; Millan, P.; Rojas, R. M. *J. Mater. Sci.* **1986**, *21*, 4411.

(25) Lorenz, M.; Kempe, G. *J. Therm. Anal.* **1984**, *29*, 581.

(26) Lee, S. H.; Her, Y. S.; Matijević, E. *J. Colloid Interface Sci.* **1997**, *186*, 193.

(27) Privman, V.; Goia, D. V.; Park, J.; Matijević, E. *J. Colloid Interface Sci.* **1999**, *213*, 36.

(28) Kannan, S.; Swamy, C. S. *J. Mater. Sci. Lett.* **1992**, *11*, 1585.

(29) Xu, Z. P.; Zeng, H. C. *Chem. Mater.* **1999**, *11*, 67.

(30) Nakamoto, K. *Infrared and Raman Spectroscopy of Inorganic and Coordination Compounds*; Wiley: New York, 1978.

(31) Busca, G.; Lorenzelli, V. *Mater. Chem. Phys.* **1982**, *7*, 89.

(32) Pozas, R.; Ocana, M.; Morales, M. P.; Serna, C. J. *J. Colloid Interface Sci.* **2002**, *254*, 87.

(33) Xu, R.; Zeng, H. C. *J. Phys. Chem. B* **2003**, *107*, 926.

(34) Feng, J.; Zeng, H. C. *Chem. Mater.* **2003**, *15*, 2829.

(35) Liu, Y.; Wang, G.; Xu, C.; Wang, W. *Chem. Commun.* **2002**, 1486.